Supporting Information

Rajimehr *et al.* 10.1073/pnas.0807304106

SI Text

FreeSurfer Analysis. For each subject, the inflated cortex and flattened cortical patches were generated based on the reconstruction of anatomical images. All functional images were motion corrected by using AFNI (1), spatially smoothed with a Gaussian kernel of 1 mm (for monkeys) or 2.5 mm (for humans) HWHM, and normalized across sessions. The average signal intensity maps were then calculated for each stimulus condition. The estimated hemodynamic response was defined by a γ function of 0 hemodynamic delay, 8-s dispersion, and gamma exponent of 0.3 (for MION response in monkeys) or 2.25-s hemodynamic delay and 1.25-s dispersion (for BOLD response in humans). The voxel-wise statistical tests were conducted by computing contrasts based on a univariate general linear model. To avoid sampling gaps in the (high-resolution) monkey fMRI, the functional activity was sampled and averaged from all voxels located within the gray matter, along the surface normal. Finally, the significance levels were projected onto the inflated/flattened cortex after coregistering the functional and anatomical slices.

Functional data were spatially normalized across sessions (in monkeys) and across subjects (in humans) by using a spherical transformation (2, 3), then averaged by using a fixed-effects model.

Caret Analysis. Cortical surfaces of an individual macaque brain and its associated fMRI data were registered to the macaque F99UA1 atlas (4) by using surface-based registration of spherical maps, as constrained by sulcal landmarks on the individual and atlas hemispheres. Similarly, cortical surfaces of the averaged human brain (the average of 10 human subjects) and its associated fMRI data were registered to the human PALS atlas (5). Finally, the monkey and human atlas surfaces were registered (deformed) to one another by using surface-based registration and a set of landmark contours for cortical areas that are strongly suspected to be homologous across species (see ref. 6 for review). In total, 23 registration landmarks were used, including three functional landmarks, which were based on an interspecies comparison of object-specific fMRI activations (7).

1. Cox RW, Jesmanowicz A (1999) Real-time 3D image registration for functional MRI. *Magn Reson Med* 42:1014–1018.
2. Dale AM, Fischl B, Sereno MI (1999) Cortical surface-based analysis. I. Segmentation and surface reconstruction. *NeuroImage* 9:179–194.
3. Fischl B, Sereno MI, Dale AM (1999) Cortical surface-based analysis. II: Inflation, flattening, and a surface-based coordinate system. *NeuroImage* 9:195–207.
4. Van Essen DC (2004) Surface-based approaches to spatial localization and registration in primate cerebral cortex. *NeuroImage* 23:S97–S107.
5. Van Essen DC (2005) A population-average, landmark- and surface-based (PALS) atlas of human cerebral cortex. *NeuroImage*. 28: 635–662.
6. Van Essen DC (2003) Organization of visual areas in macaque and human cerebral cortex. *The Visual Neurosciences*, eds Chalupa L, Werner JS (MIT Press, Cambridge, MA), pp 507–521.
7. Denys K, *et al.* (2004) The processing of visual shape in the cerebral cortex of human and nonhuman primates: A functional magnetic resonance imaging study. *J Neurosci* 24:2551–2565.
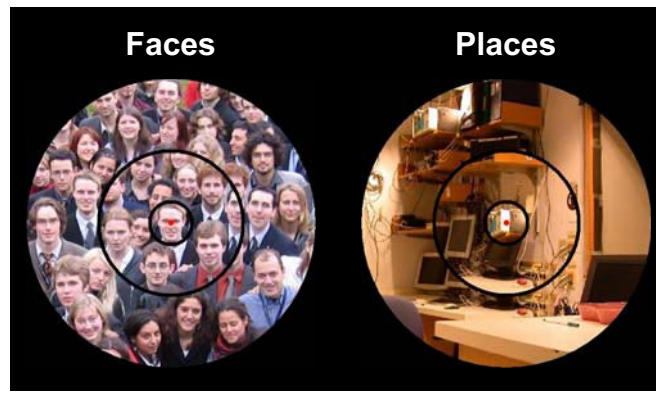
Fig. S1. The initial stimuli used for face/place mapping in macaques and humans. The stimuli included face- and place-based images, which were confined to retinotopically-specific ring apertures. The ring-shaped apertures were located in 3 eccentricities of the visual field (fovea, midperiphery, and periphery).
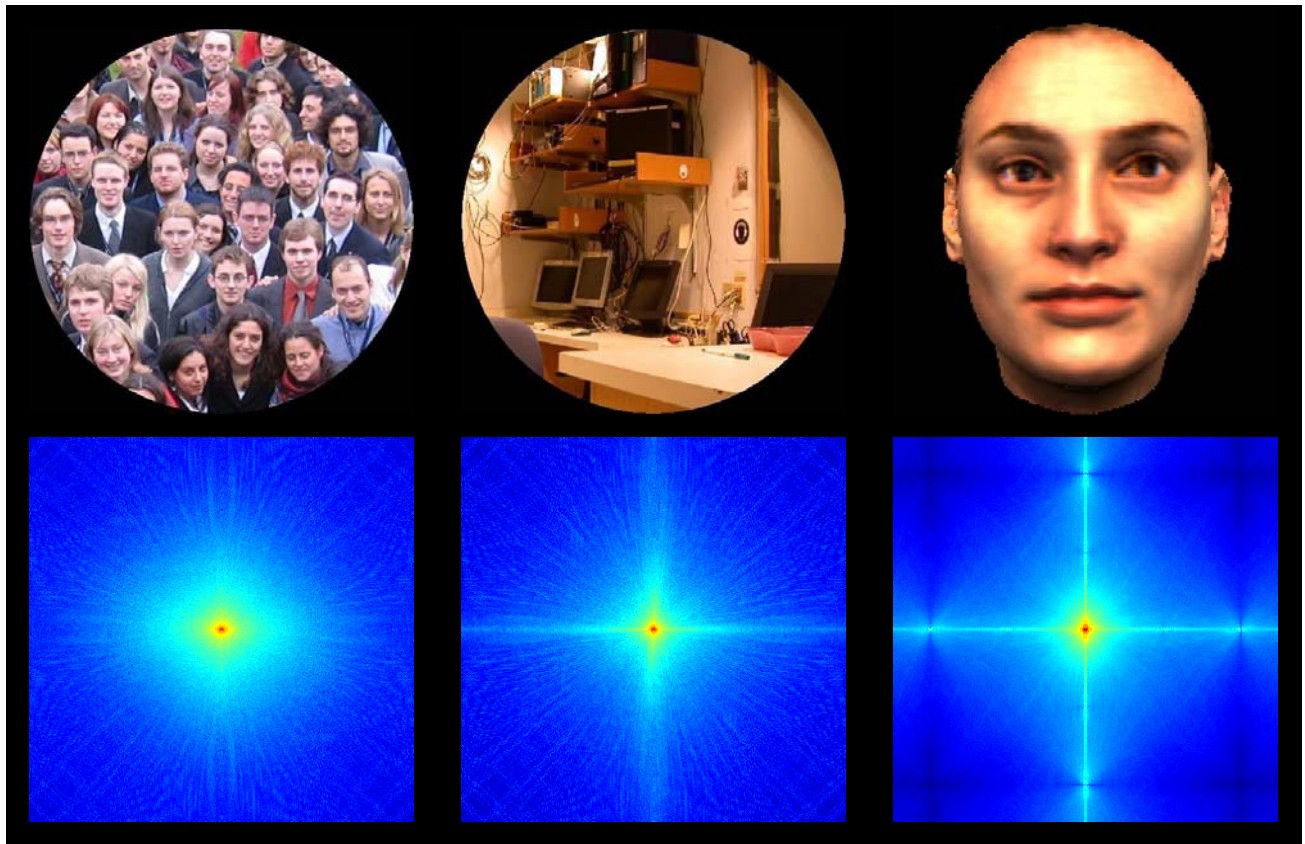
Fig. S2. Fast Fourier transform (FFT) of face and place images. (*Upper*) Sample images of group photo face stimuli (*Left*), place stimuli (*Center*), and (as control) single face stimuli (*Right*). Single face images were selected from the Max-Planck face database, and their size was roughly equated to the size of other face and place images. (*Lower*) The averaged 2D FFT of 10 group photo face (*Left*), 10 place (*Center*), and 30 single face (*Right*) images. The red/blue color map represents the FFT magnitude (magnitude = red > yellow > cyan > blue) in Fourier space (the center of Fourier space indicates zero spatial frequency). The spatial frequency distributions of group photo faces and places were qualitatively similar to each other, but the spectral distribution of the single face stimuli was different. Quantitatively, the normalized correlation between FFT magnitudes of group photo face and place images was significantly greater than that between FFT magnitudes of single face and place images ($P < 0.0001$; t test). This analysis suggests that group photo face stimuli are more optimal for the face-vs.-place comparison.

Fig. S3. Full-screen stimuli also activate human ATFP. In an additional face/place localizer experiment, the full-screen stimuli were used for mapping face patches in humans. Activation maps are displayed on the ventral view of the inflated right and left hemispheres in a representative subject. The human ATFP was significantly activated even with these more conventional stimuli. The maps also show typical FFA activity in the ventral occipito-temporal cortex. The map threshold is $P < 10^{-2}$.

Fig. S4. Examples of face and object stimuli used in the face/object localizer experiment. M, male faces; F, female faces; G, graspable objects; NG, nongraspable objects.

Fig. S5. The location of human ATFP in different anatomical slices of the human brain. The ATFP (as localized by faces versus objects) is shown in coronal, horizontal, and sagittal slices in a representative subject. The Talairach coordinates of the peak activity in ATFP are 38.4, −5.0, −27.0.

Fig. S6. fMRI activation in human ATFP for faces and objects. In this ROI analysis, the ATFP was localized based on face/place data (an independent localizer) in 5 human subjects who reliably showed this face patch in their maps, and then the fMRI activation in the ATFP was calculated for faces and objects in the same subjects. The ATFP activity for faces was significantly greater than that for objects, in both odd and even functional runs ($P < 0.05$; t test). The error bars indicate 1 SEM, measured across subjects.
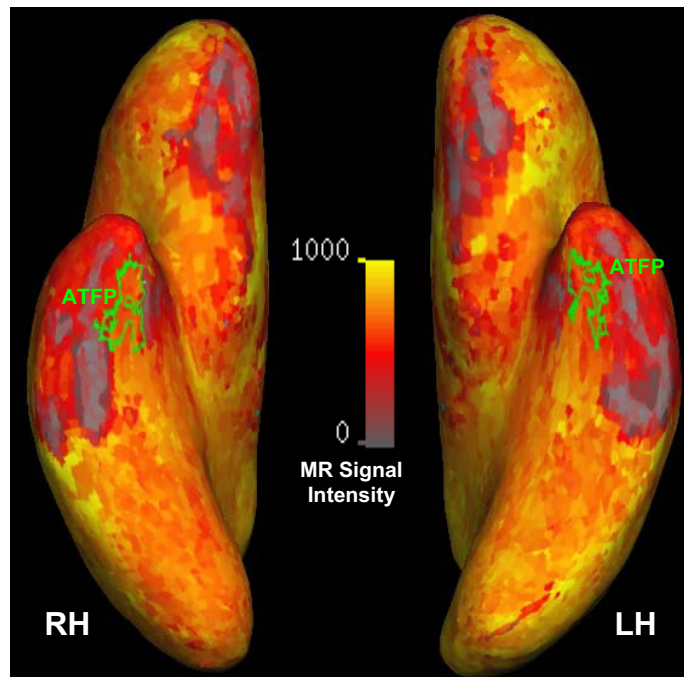
Fig. S7. Signal drop-out in anterior temporal lobe. The maps show MR signal intensity values in raw functional volumes, overlaid on the inflated surface in a representative human subject. The signal intensity maps show signal drop-out in anterior inferotemporal cortex, where human ATFP is located (see Fig. S3 for the face/place map in this subject).